KfK 4319
September 1987

IVA 2 Application: Three Dimensional Effects During APWR LOCA

N. I. Kolev
Institut für Neutronenphysik und Reaktortechnik

Kernforschungszentrum Karlsruhe

KERNFORSCHUNGSZENTRUM KARLSRUHE
Institut für Neutronenphysik und Reaktortechnik

KfK 4319

IVA2 Application: Three Dimensional Effects During APWR LOCA

N.I. Kolev

Kernforschungszentrum Karlsruhe GmbH, Karlsruhe

Kernforschungszentrum Karlsruhe GmbH
Postfach 3640, 7500 Karlsruhe 1

ISSN 0303-4003

Abstract

Using the IVA2/005 computer code three dimensional effects during a LOCA for a homogeneous APWR are simulated. The formation and transport of void and droplets in a reactor vessel of the KWU-1300 type, responsible for the three-dimensional cooling of the core are shown as functions of time and space. The results prove that it is important to perform a three-dimensional analysis rather than a one-dimensional one to predict more realistic temperature distributions of the fuel rods, especially for the strong three-dimensional multi-velocity fields considered in this study.

IVA2 Anwendung: Dreidimensioanle Effekte während einer FDWR-LOCA.

Zusammenfassung

Mit Hilfe des Computerprogramms IVA2/005 wurden dreidimensionale Effekte während eines LOCA für einen homogenen FDWR simuliert. Dampf-, Tröpfchenbildung und deren Transport in einem KWU-1300 Reaktordruckgefäß, verantwortlich für die dreidimensionale Kühlung der Spaltzone, sind als Funktionen der Zeit und des Orts gezeigt. Die Ergebnisse beweisen, daß es für die Vorhersage realistischer Temperaturverteilungen in den Brennstäben der Spaltzone wichtig ist dreidimensioanle Analysen anstatt eindimensionaler durchzuführen, insbesondere für ausgeprägte dreidimensionale Strömungen mit mehr als zwei Geschwindigkeitsfeldern, die in dieser Untersuchung betrachtet wurden.

Table of contents page

1. Introduction 1

2. Computational model, initial and boundary conditions 1

3. Results and discussion 3

4. Conclusions 5

5. References 7

1. Introduction

In order to increases the fuel utilization using the achieved technical standard of the light water reactor technology the suggestion by Edlund /1/ attracts the attention of nuclear engineers since a decade. The idea was to replace the core of a pressurized water reactor (PWR) by a core formed by fuel rods with a tight lattice. Increasing the Pu-concentration in the core and reducting the water volume fracton results in conversion ratios of 0.8 to 0.9% compared to 0.5 to 0.6 for the PWR technology, which means increasing the uranium utilization by up to 4. /2,3/. The important results of the work performed in the Karlsruhe Nuclear Center on neutron physics and thermal-hydraulic design of an advanced pressurized water reactor (APWR) is described in /2,3/. The next step is to investigate the behavior of an APWR during postulated accidents. The results of such investigations for a loss of coolant accident (LOCA) and anticipated transients without scram (ATWS) using RELAP5/Mod1 (Ispra version) for homogeneous and heterogeneous KFK-APWR design are reported in /4/.

The use of an one dimensional representation of the vessel for numerical simulation a LOCA raised some questions, e.g.

- can the downcomer be divided into two tracts without interactions belonging to the broken and intact loops,
- can the core region be divided in sectors without interaction in order to simulate the three dimensional effect of the water injection into the upper plenum and its transport through the core, etc.

The purpose of this paper is to give answers on such questions.

2. Computational model, initial and boundary conditions

We use, as an example, the RELAP5/Mod1 LOCA simulation of a heterogeneous APWR reported in /4/ (double ended break between the main water pump and reactor). The obtained

- mass flow in the reactor entrance, outlet and ECCS nozzles and
- the thermodynamical properties belonging to the mass flows mentiond

are used as boundary conditions for the IVA2/005 simulation discussed in this paper.

The IVA2 computer code is a three phase, three component flow analyser. The flow is described by means of three-velocity fields in thermal and mechanical nonequilibrium in cylindrical geometry with arbitrary internals including a nuclear reactor core if desired. Details about the code can be obtained in /5-11/.

The only degree of freedom compared to the RELAP-calculation was the boundary condition on the broken outlet nozzle. The atmospheric pressure is used as a boundary condition at this place. The vessel and core geometry summarized in Table 1 is taken from /2/.

Table 1: Reactor Parameter (homogeneous KfK APWR design /2/).

Parameter	Size
Power (MW(thermal))	3954
Pressure outlet nozzle (MPa)	16.3
Volumetric flow rate (m^3/s)	35
Entrance coolant temperature (K)	563.65
Number of fuel rods	94210
Outer diameter, fuel (m)	0.0095
Outer diameter, pellet (m)	0.0085
Clad thickness (m)	0.0004
Pitch, triangular geometry (m)	0.0114
Core height (m)	2.2
Downcomer i.d. (m)	4.2
Vessel i.d. (m)	5
Vessel height (m)	6.8
Distance between vessel bottom and core bottom (m)	1

The vessel geometry corresponds closely to the standard vessel design of a 1300-MW (thermal) KWU PWR. The radial and the axial power distribution is taken also from /2/ (radial form factor = 1.023, axial form factor = 1.32). The accident starts at a reactor power 6% higher than the nominal. The ANS Standard Curve for fission product decay heat is assumed as in the RELAP-simulation /4/. During the LOCA period the four low pressure and four high pressure emergency cooling pumps are not yet in operation /4/.

Figures 1 and 2 show the descretisation of the vessel by 1656 computational cells (9 radial 23 axial 8 azimuthal) to represent the complicated vessel geometries

including the internals. The used idealization of the vessel geometry for the inlet and outlet nozzle is shown in Fig.2.

The initial steady state was computationally obtained by increasing the inlet flow rate within 5 s from zero to the nominal value. The thermal power input was jumpwise increased in the 5-th s from zero to 106% of the nominal value. Shortly after the 17-th second the steady state was reached. The obtained steady state distribution of the maximal fuel temperature, cladding surface temperture and pressure as a function of (r,z) space for the first angular sector (J = 2) are presented in Figs.3 through 5a).

3. Results and discussion

Figure 5 show the pressure distributions as a function of (r,z) for the vertical plane J = 2. This plane contains the outlet nozzle belonging to the broken loop. The time is used as a parameter. Figure 5a) shows the pressure distribution at steady state. From the pressure distribution in the milliseconds region three dimensional loads of the vessel internals are obtained which is not possible with one dimensional codes. The maximum pressure difference inside the vessel is clearly seen. Fig.5b), shows the pressure distribution after 20 ms. One can see that the maximum pressure difference acting on the thermal shield is 7.69 MPa in that time. This pressure difference decrease with the time to 0.071 MPa after 25.7 s and and to 0.039 MPa at the end of the simulated process, respectively. The smooth pressure distributions inside the vessel as shown in Figs.5a) and b) is typical for the time before the cold water from the ECCS reaches the upper plenum and the core. Thereafter the intensive vapor production in the core results in not smooth pressure distributions as shown in Figs.5c) and d).

Figure 6 shows the maximum and the minimum pressure predicted by IVA2 during the transient, compared with the RELAP5/Mod1 prediction. Within the first 3 seconds the RELAP5/Mod1 prediction is within the minimum and maximum pressure predicted by IVA2. Between 3 and 21 s IVA2 predicts faster and after 21 s slower depressurization than RELAP5/Mod1.

Figure 7 shows the void fraction in the vessel as a function of (r,z) for the plane J = 5. This is the plane where one of the two ECCS inlet nozzles enters the vessel. The time is used as a parameter. An important phenomenon can be recognized from these figures. After the first second the vapor, formed by spontaneous

flashing and evaporation in the core, is carried out of the core in the predominant flow direction. The vapor generating core has a considerable resistance for the vapor in the lower plenum on the way upwards. Further, the bubbles in the upper part of the core and in the upper plenum change their direction do to the decreasing of the center of mass (c.m.) velocity in the core. Thus void package is formed in the upper plenum, too. After 4 seconds, almost the total vessel is occupied by steam. Only the bypass region and its neighborhood have a considerable liquid concentration. After the 7-th second, the liquid fraction in the bypass region is decreasing. In the central region the rest of the liquid is divided into film and droplets. The heat transfer logic of IVA2 predicts film boiling in the core either by a DNB-correlation (Bowring in this simulation) or if the liquid film thickness becomes less than 0.01 mm. Comparing the void fraction of Fig.7 with the fuel clad surface temperature, presented in Fig.8, we see that the core is good coolable until 15 sec. During that time some places in the core are cooled by film boiling forced convection. The time between 15 and 24s is characterized by a two phase flow through the core consisting mainly of steam and droplets. The considerable deposition depending on the local conditions change the cooling mechanism in different places and at different times. From such kind of simulation one can not say that at given point in the core and at a given moment the real temperature will be the predicted one, but one can recognize the character of the frequently changing local condition in the three dimensional space with predominant one or other cooling mechanism. After 24 s, cool water from the ECCS is entered into the upper plenum. So the cooling mechanism is changed from predominant film boiling to the predominant two-phase forced convection in 30-th second. At that time, the outer region on the side of the ECCS injection is better cooled than the central region. From Fig.7 one can clearly see that the resistance of the evaporated central part of the core is much higher for the entering liquid. So the liquid occupies mainly the outer region. At that time a considerable portion of the entrained liquid is carried out by the steam flow, without taking part in the contact core cooling. From Fig.7 one can destinguish the cyclic character of the initial phase of the upper core reflooding process within the time from 28 to 33 s, characterized by forced two phase convection replaced locally by film boiling or predominant steam convection ect. This impression is supported by analyzing Fig.8 for the same time interval. The interaction between the bypass region, having much liquid, and central core region is clearly shown in Fig.7. Therefore, dividing the core into two not interacting parts for a one dimensional simulation as discussed in /4/ is somewhat arbitrary but conservative. Figure 9 shows a

comparison between the maximum fuel cladding temperature predicted by RELAP5/Mod1 for a hot spot with a hot channel factor equal to 2.57, compared with the IVA2 prediction of the maximum and minimum cladding surface and fuel rod temperatures. In general, IVA2 predicts temperatures less than RELAP5/Mod1 for the considered 33 seconds of the LOCA. The maximum form factor for the IVA2 simulation of 1.35 is the one of the reasons. The other reason is the more realistic three dimensional flow simulation by means of three velocity fields and much detailed representation of the core internals by IVA2 simulation. This statement is supported by PWR-LOCA calculation using COBRA/TRAC and TRAC reported in /12,13/ respectively.

The difference between the maximum fuel and cladding temperatures is very small after the first second. That leads to the conclusion that the radial heat conduction in the fuel rod can be simulated using simply one cylinder (compared to 5 radial discretisation points in IVA2 fuel model).

Figure 10 shows a vector plot of a center of mass velocity for the plane J = 3. This is the vertical plane next to the plane connected with the broken loop. The figure shows that within the first 18 ms the core flow is not yet inverted. After the first second, the flow in the core and lower plenum is becoming inverted, but not the flow in the upper plenum. The flow inversion in the upper plenum starts in the first second and finishes somewhere in teh 18-th second. Some recirculation is observed in the upper plenum in the 5-th and 24-th seconds. It is very interesting to see the non-uniform c.m. velocity distribution in the core e.g. the stagnation in the upper core part within 21-th and 24-th seconds. The velocity in the lower right corner changes its direction. That is the reason of droplet separation in this region observed in the Fig.7.

4. Conclusion

It is obvious that the detailed description of the three-dimensional vessel internals and two-phase flow details during a LOCA compared with a one dimensional representation gives much more realistic and useful information. This conclusion is not new. New is, for an engineer, the available computational power of the modern computers, making such very complicated two-phase flow simulations possible at an acceptable price. The representation of the large scale reactor vessel during LOCA-simulation by quasi one dimensional channels, with or without interaction, is no longer necessary. The discussion whether such kind

of representation is conservative or not is less important for the theoretical reactor safety analysis now-a-day because a new generation of three dimensional computer codes is available and can be used for more realistic analyses. But the important question, how accurate is the prediction of such multidimensional complicated flow processes by code like IVA2 can be answered only be comparison with well-instrumented multidimensional experiments. The number of successful comparisons of separate effects modelled with the IVA2 constitutive package preceding this study /6,9/, together with the successful comparison of the IVA2 prediction of none adiabatic two phase flow in reactor geometry /7/ and strongly nonhomogeneous adiabatic two phase flow in cylindrical geometry with internals /10,11/ give some confidence, that the simulation presented above give a realistic picture of the important characteristics and trends during a APWR-LOCA for the used boundary conditions. Large scale multi dimensional experiments are further needed in order to make such predictions more accurate in the future.

5. References

/1/ Edlund M.C.: High Conversion Ratio Plutonium Recycle in Pressurized Water Reactors, Ann. Nucl. Energy, 2, 801 (1975).

/2/ Broeders C.H.M. and Dalle Donne M.: Auslegung eines heterogenen bzw. homogenen $(Pu,U)O_2$-Kerns mit einem Brennstabgitter für einen fortgeschrittenen Druckwasserreactor (FWR), KfK-Nachrichten, Vol. 17, p.140, Kernforschungszentrum Karlsruhe (1985).

/3/ Broeders C.H.M., Dalle Donne M.: Computational Design of a $(Pu,U)O_2$ Core With a Tight Fuel Rod Lattice For An Advanced Pressurized Light Water Reactor, Nuclear Technology Vol.71 Oct. 1985, pp.82-95.

/4/ Dalle Donne M., Ferrero C.: LOCA and ATWS Calculations for Homogeneous and Heterogeneous Advanced Pressurized Water Reactors, subm. to Nucl. Technolgy 1987.

/5/ Kolev N.I.: Transient Three-Dimensional Three-Phase Three-Component Nonequilibrium Flor in Porous Bodies Described by Three-Velocity Fields, Kernenergie 19 (1986) 10 pp.383-392 or in German in KfK 3910, März 1985.

/6/ Kolev N.I.: Transient Three-Phase Three-Component Nonequlibrium Nonhomogeneous Flow Described by a One-Dimensional Slip Model, Atomkernenergie, Kerntechnik Vol.49 (1987)No.4, or in German in KfK 3926, August 1985.

/7/ Kolev N.I.: A Three-Field Diffusion Model of Three-Phase, Three-Component Flow For the Transient Three-Dimensional Computer Code IVA2/001, Nuclear Technology, Vol.78 August 1987 pp. 95-131, or in German in KfK 4080, Mai 1986.

/8/ Kolev N.I.: IVA2 Ein Computerprogramm zur Modellierung transienter 3D-Dreiphasen Dreikomponenten Strömungen mittels drei Geschwindigkeits-feldern in zylindrischer Geometrie mit beliebigen Einbauten einschließlich der Spaltzone eines PWR/BWR, KfK 4088, Juni 1986.

/9/ Kolev N.I.: Transiente Zweiphasen-Strömung, Springer-Verlag, Berlin, Heidelberg, New York, Tokyo 1986.

/10/ Kolev N.I.: IVA2 Verification: Expansion Phase in SNR Geometry, KfK 4310, August 1987.

/11/ Kolev N.I.: IVA2 Verification: High Gas Injection in Liquid Pool, to be published 1987.

/12/ Takeuchi K., Yang M.Y..: An implicit method for WCOBRA/TRAC, Int. Top. Meeting on Advances in Reactor Physics, Mathematics and Computation, 27-30 April 1987, Paris - France Vol.3, pp. 1853-1864.

/13/ Plank H., Winkler F.: Einfluß Mehr-Dimensionaler Strömungsvorgänge auf das Kernverhalten eines 1300 MW KWU-Druckwasserreaktors im Fall eines hypothetischen großen Kühlmittelverluststörfalls, Tagungsbericht Jahrestagung Kerntechnik 1987, Karlsruhe, pp. 207-210.

Text of the Figures

Fig.1 Cell noding diagram for the APWR vessel.

Fig.2 Idealizing of the vessel geometry for the inlet and outlet nozzles.

Fig.3 Maximum fuel rod temperature (K) in the (r,z)-plane J = 2. Steady state.

Fig.4 Cladding surface temperture (K) in the (r,z)-plane J = 2. Steady state.

Fig.5 Pressure (bar) in the (r,z)-plane J = 2. Parameter - time.

Fig.6 The maximum and the minimum vessel pressures as a function of the time predictd by IVA2, compared with RELAP5/Mod1 prediction.

Fig.7 Void fraction in the (r,z) plane J = 5 conncected with the one of the two ECCS inlet nozzles. Parameter - time.

Fig.8 Cladding surface temperature in the (r,z)-plane J = 2 connected with the broken loop.

Fig.9 The maximum and the minimum fuel- and cladding surface temperatures as a function of the time. IVA2 prediction with a form factor = 1.35 compared with the RELAP5/Mod1 prediction of the hot spot temperature (hot channel factor = 2.57).

Fig.10 The center of mass velocity in the (r,z)-plane J = 3 next to the plane connected with the broken loop.

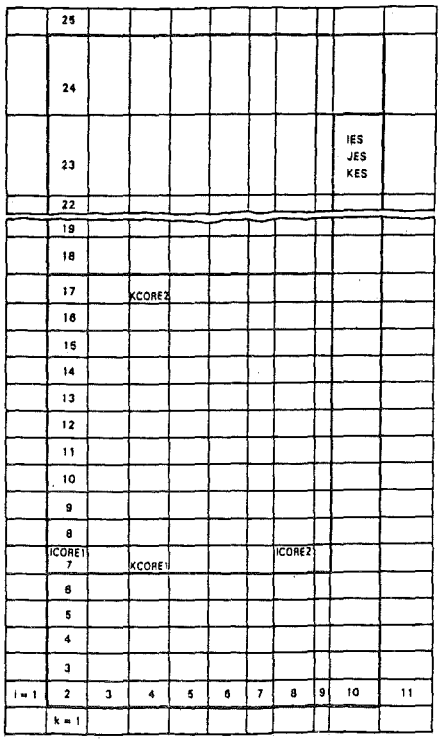

Fig.1 Cell nodding diagram for the APWR vessel.

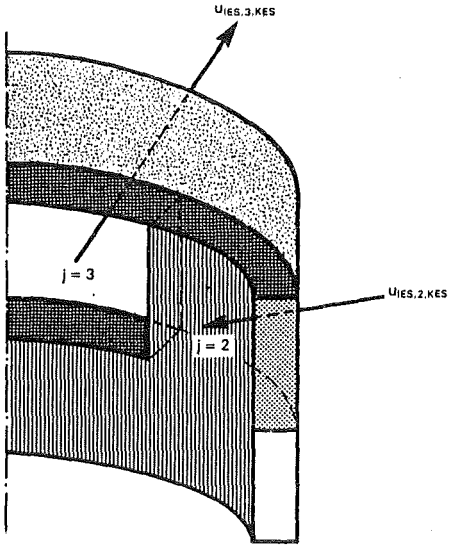

Fig.2 Idealizing of the vessel geometry for the inlet and outlet nozzles

IVA2/005 (FDWR-1300, LOCA)

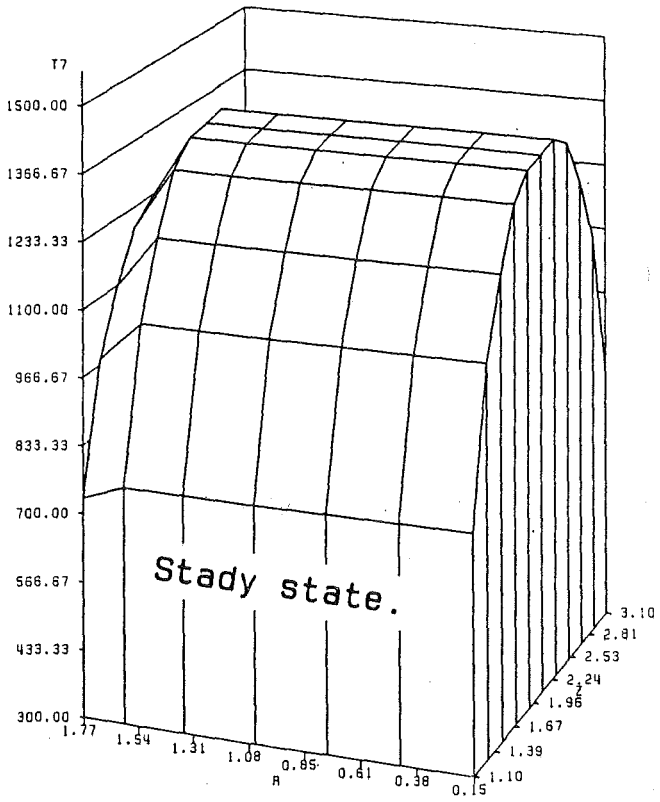

Fig.3 Maximum fuel rod temperature (K) in the (r, z) -plane J=2.

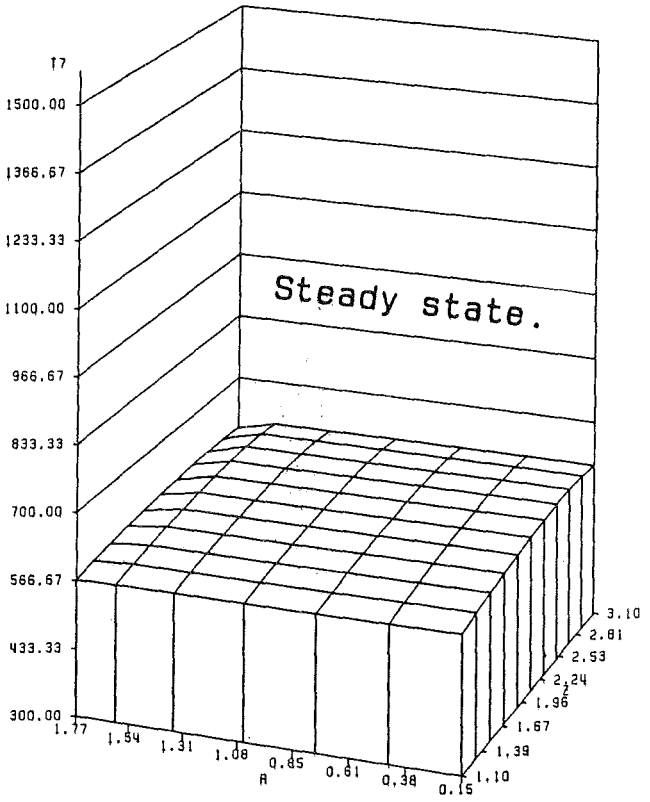

Fig.4 Cladding surface temperature (K) in the (r, z) -plane J=2.

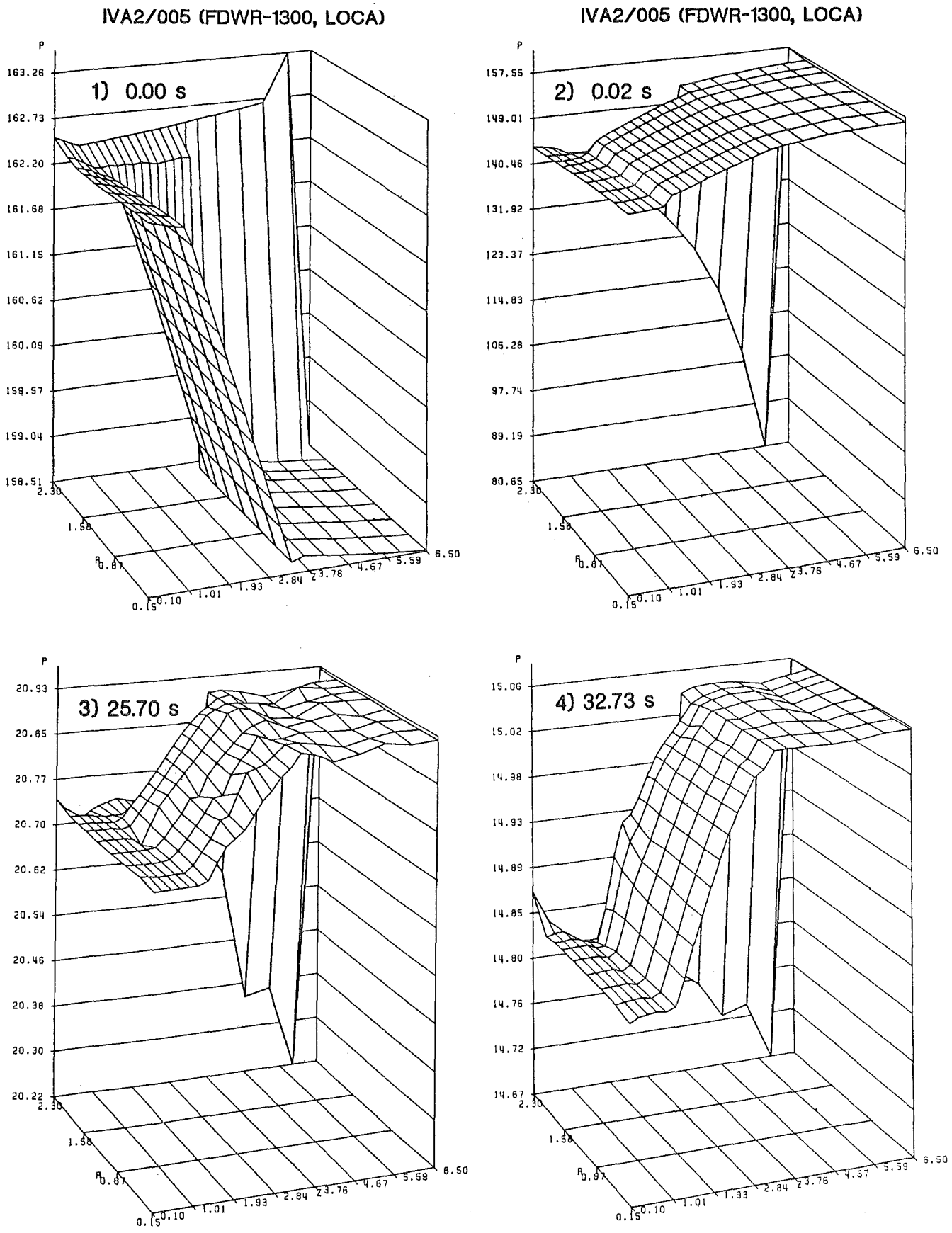

Fig.5 Pressure (bar) in the (r, z)-plane J=2. Parameter - time.

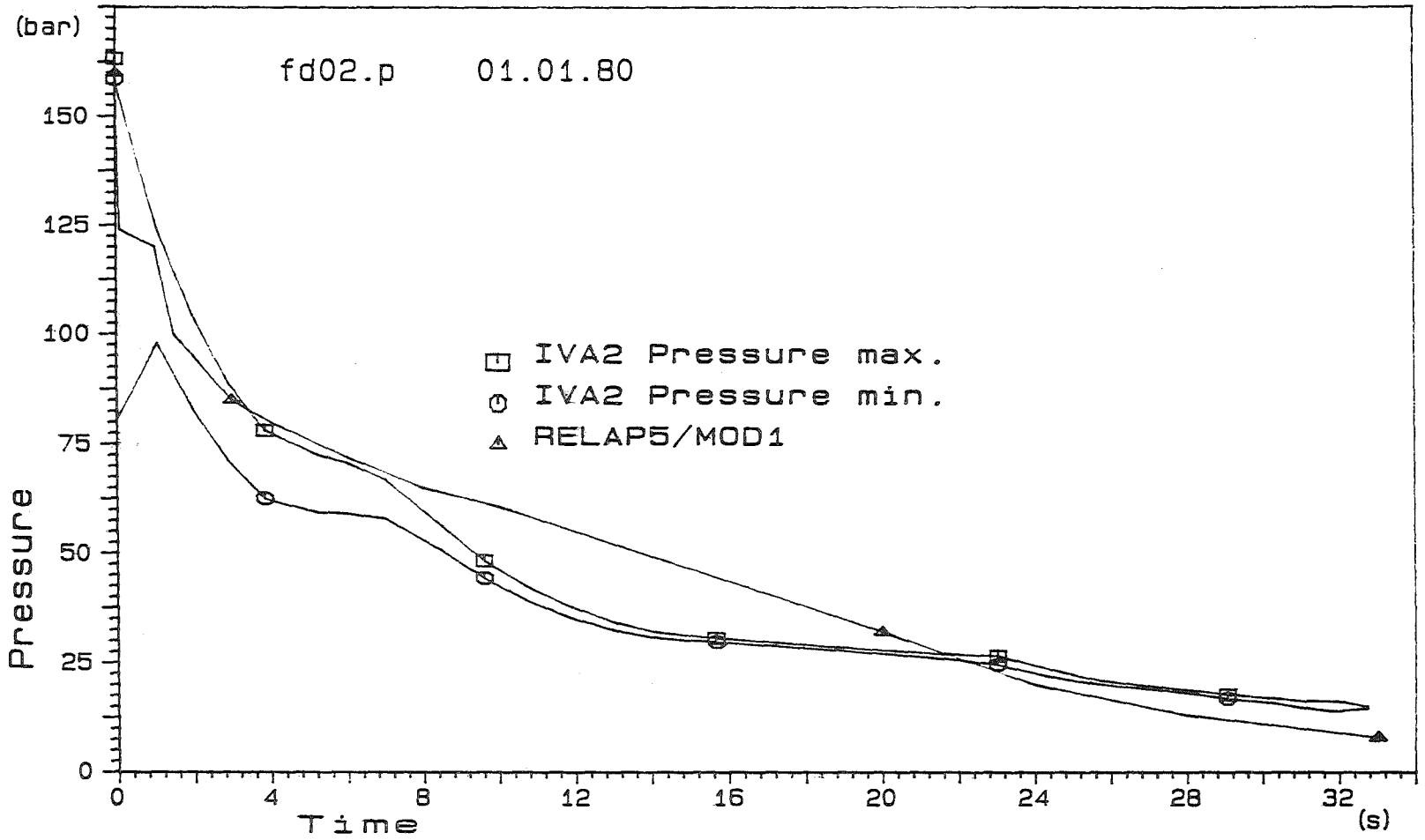

Fig.6 The maximum and the minimum vessel pressure as a function of the time predicted by IVA2, compared with RELAP5/Mod1 prediction.

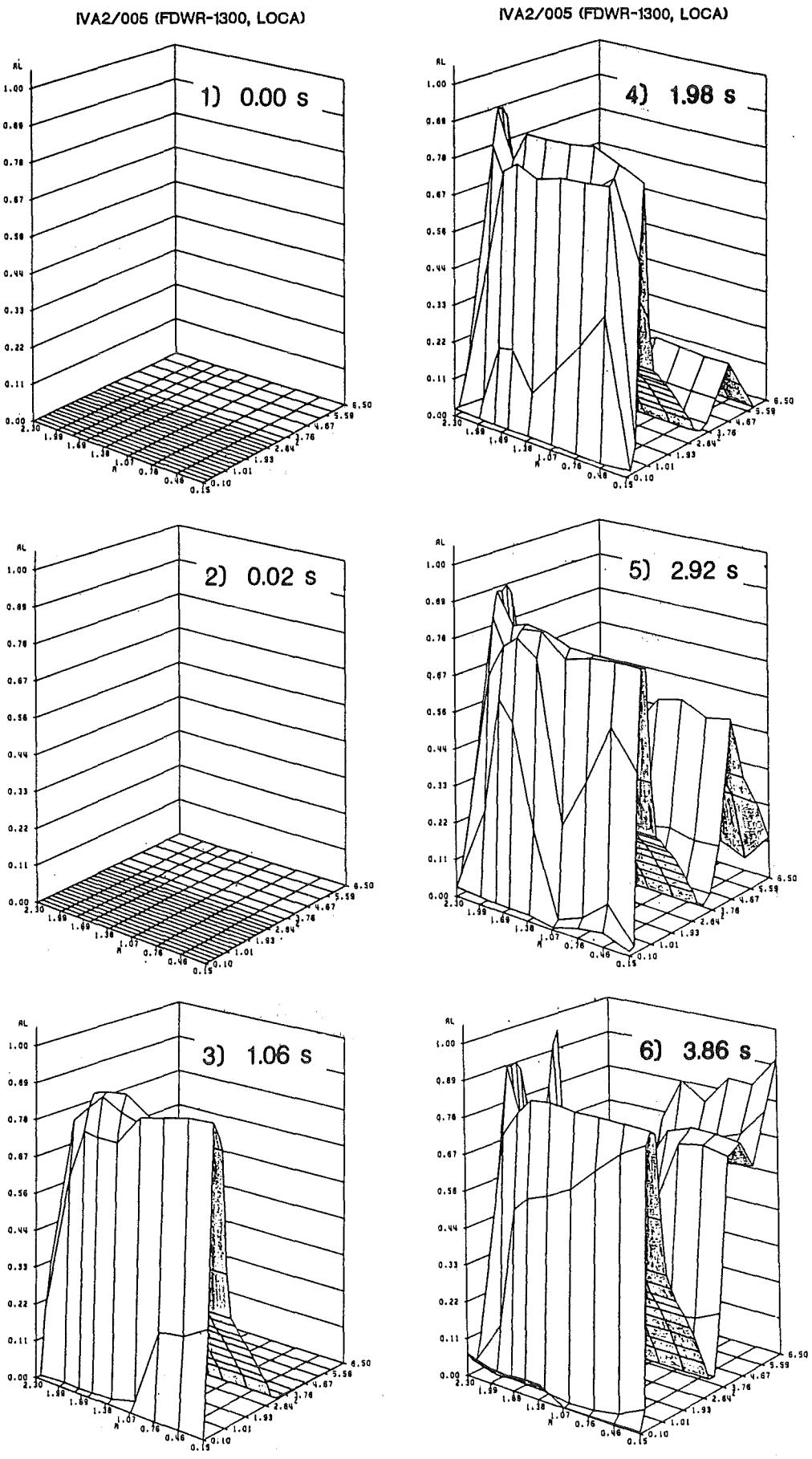

Fig.7 Void fraction in the (r, z)-plane J=5 connected with the one of the two ECCS inlet nozzles. Parameter - time.

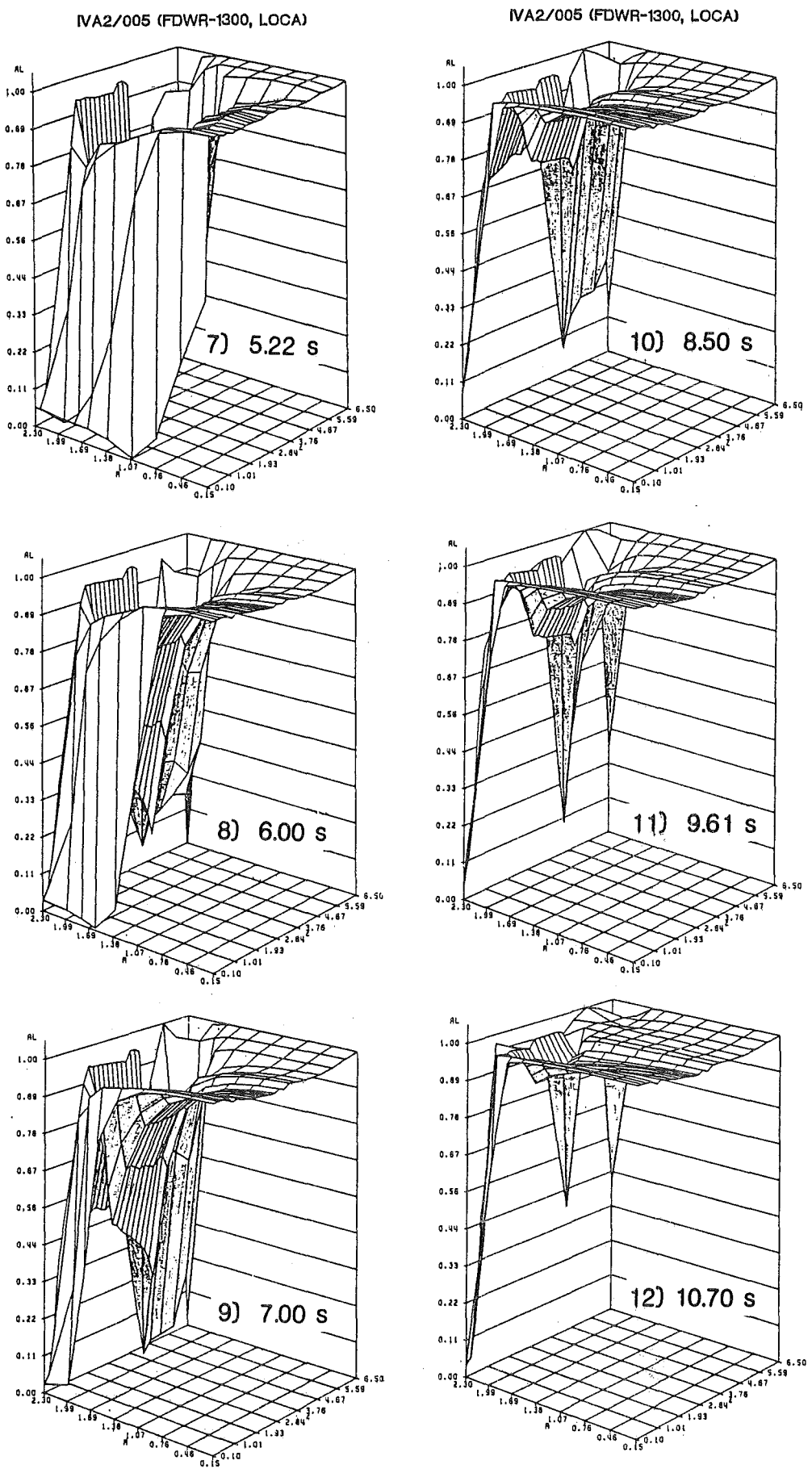

Fig.7 Void fraction in the (r, z)-plane J=5 connected with the one of the two ECCS inlet nozzles. Parameter - time.

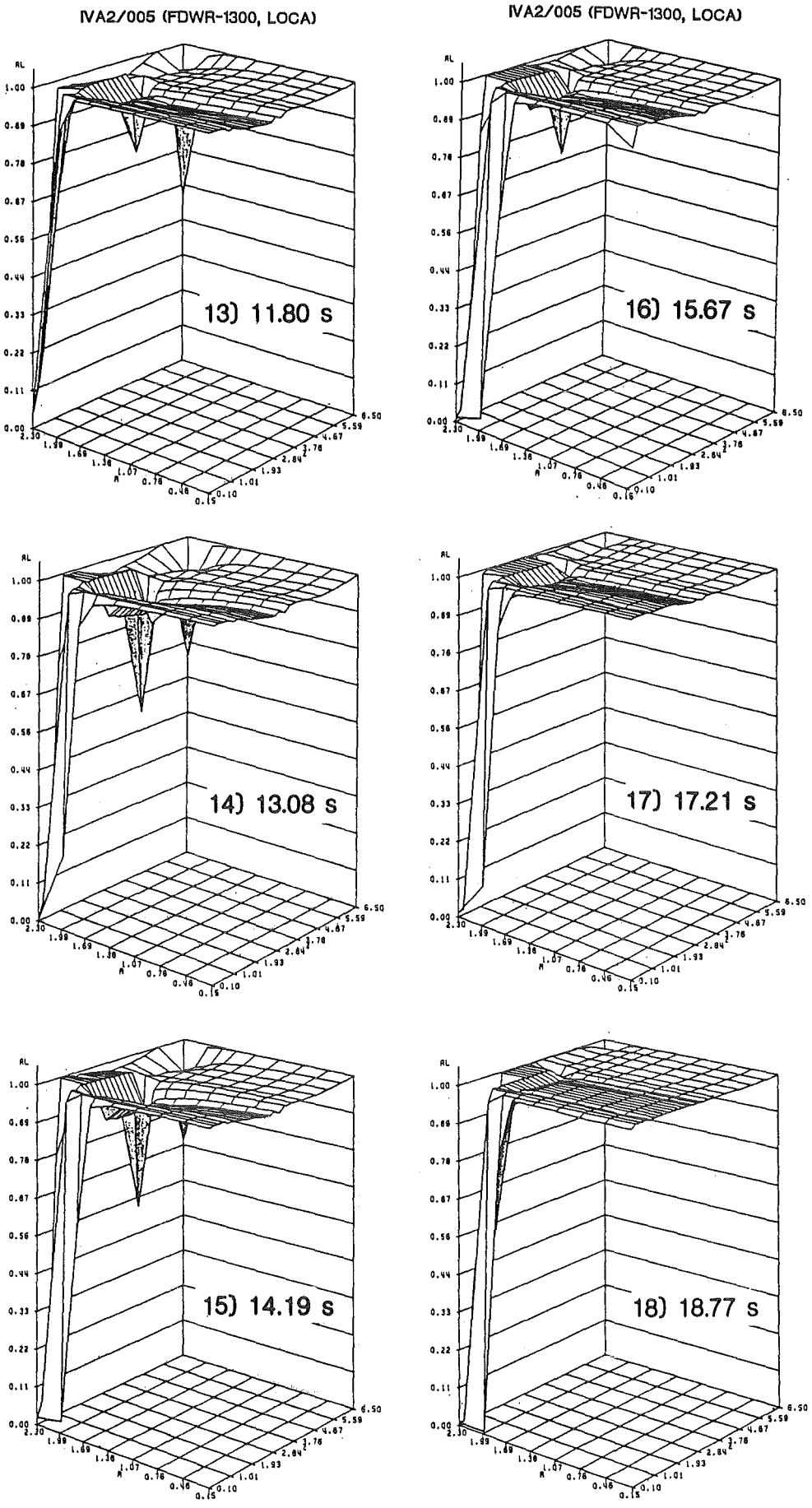

Fig.7 Void fraction in the (r, z)-plane J=5 connected with the one of the two ECCS inlet nozzles. Parameter - time.

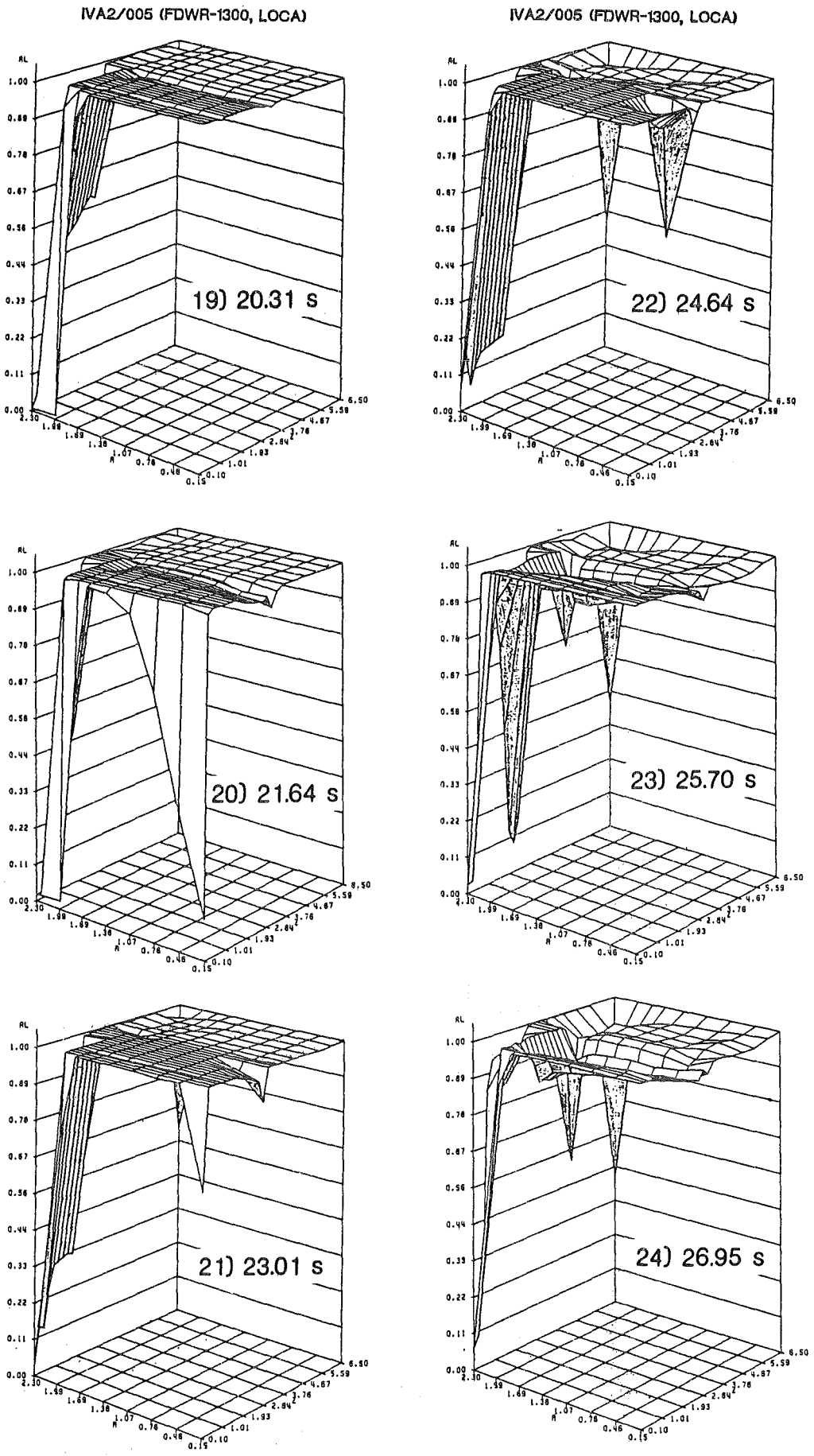

Fig.7 Void fraction in the (r, z)-plane J=5 connected with the one of the two ECCS inlet nozzles. Parameter - time.

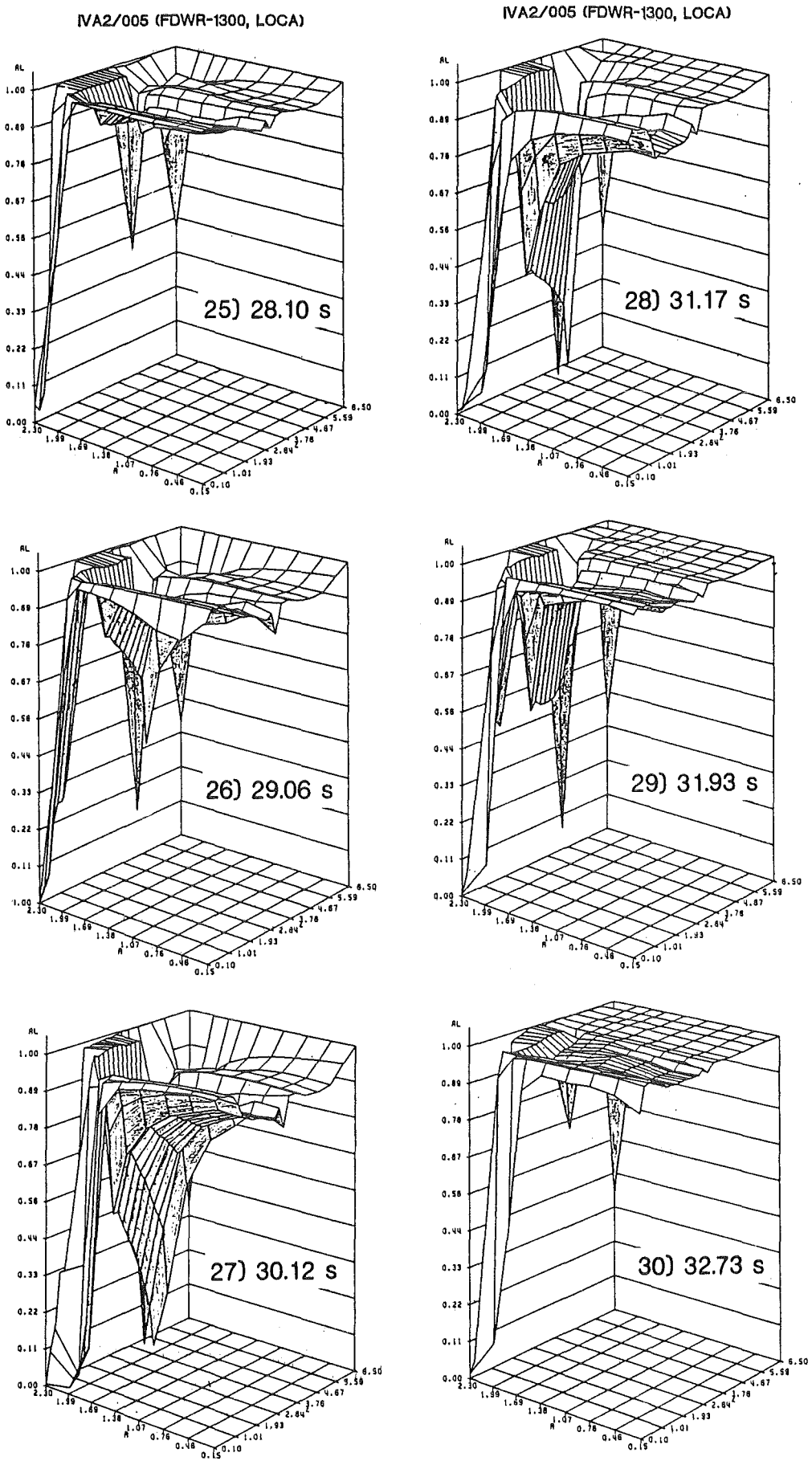

Fig.7 Void fraction in the (r, z)-plane J=5 connected with the one of the two ECCS inlet nozzles. Parameter - time.

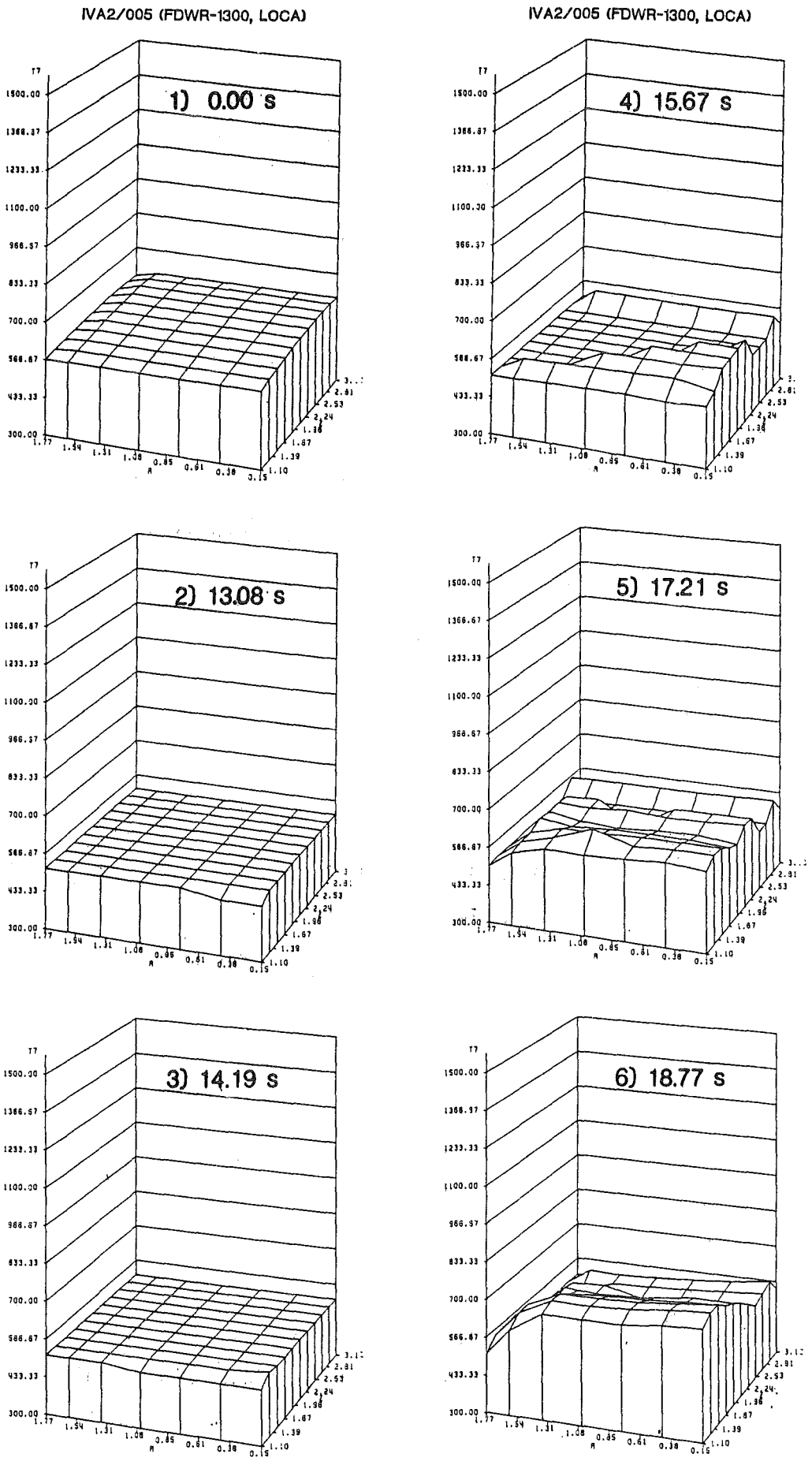

Fig.8 Cladding surface temperature in the (r, z)-plane J=2 connected with the broken loop.

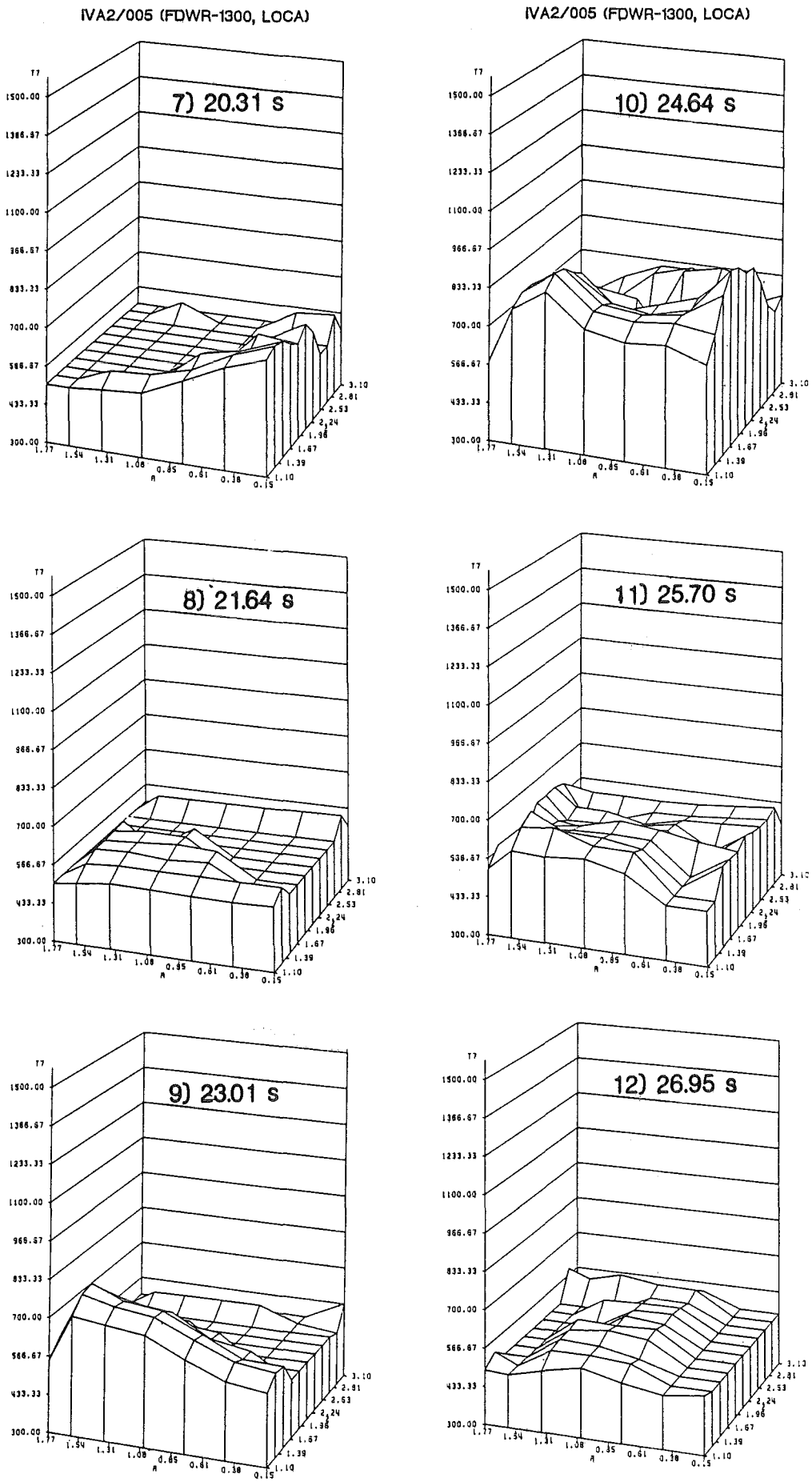

Fig.8 Cladding surface temperature in the (r, z)-plane J=2 connected with the broken loop.

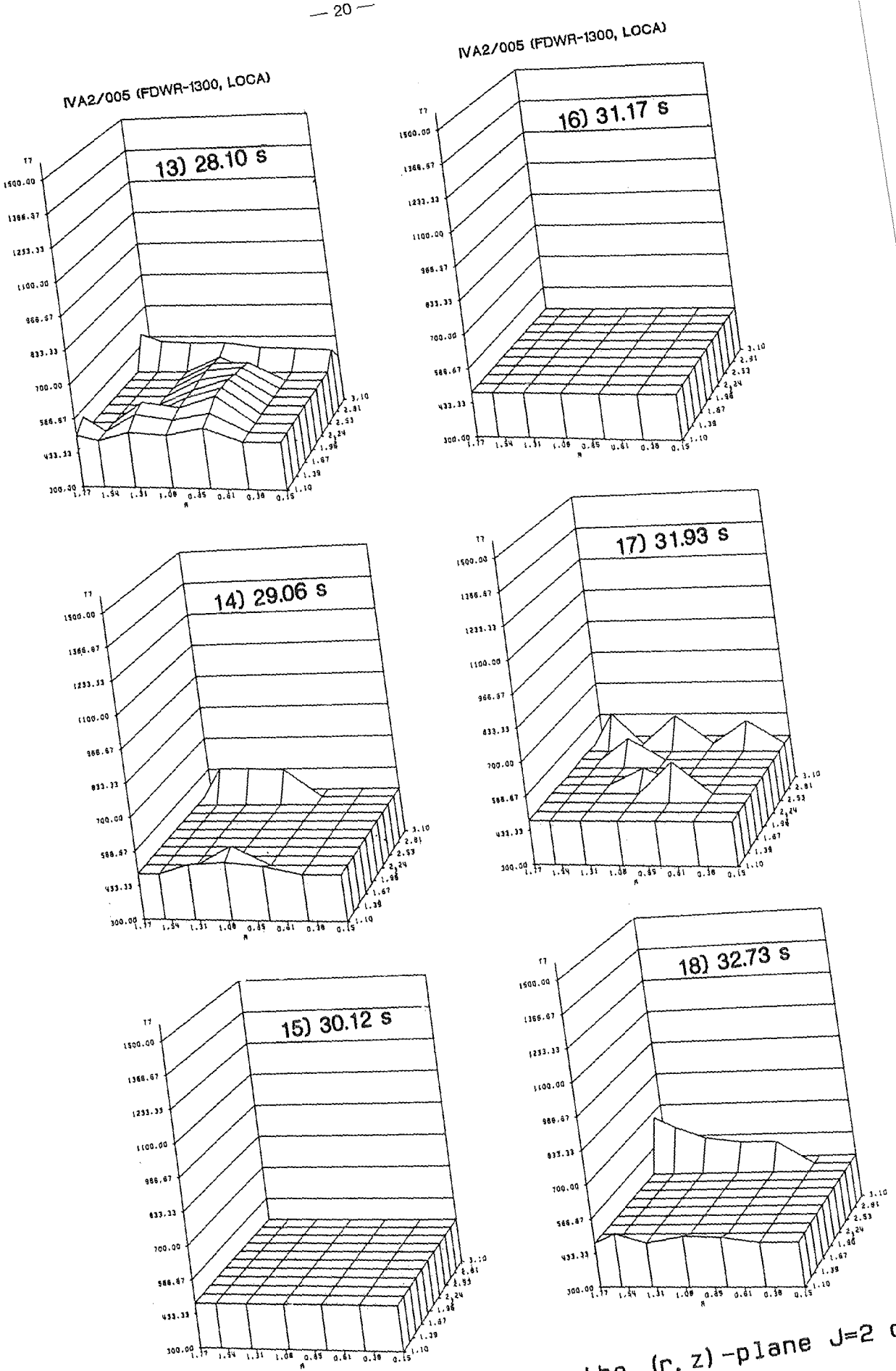

Fig.8 Cladding surface temperature in the (r, z)-plane J=2 connected with the broken loop.

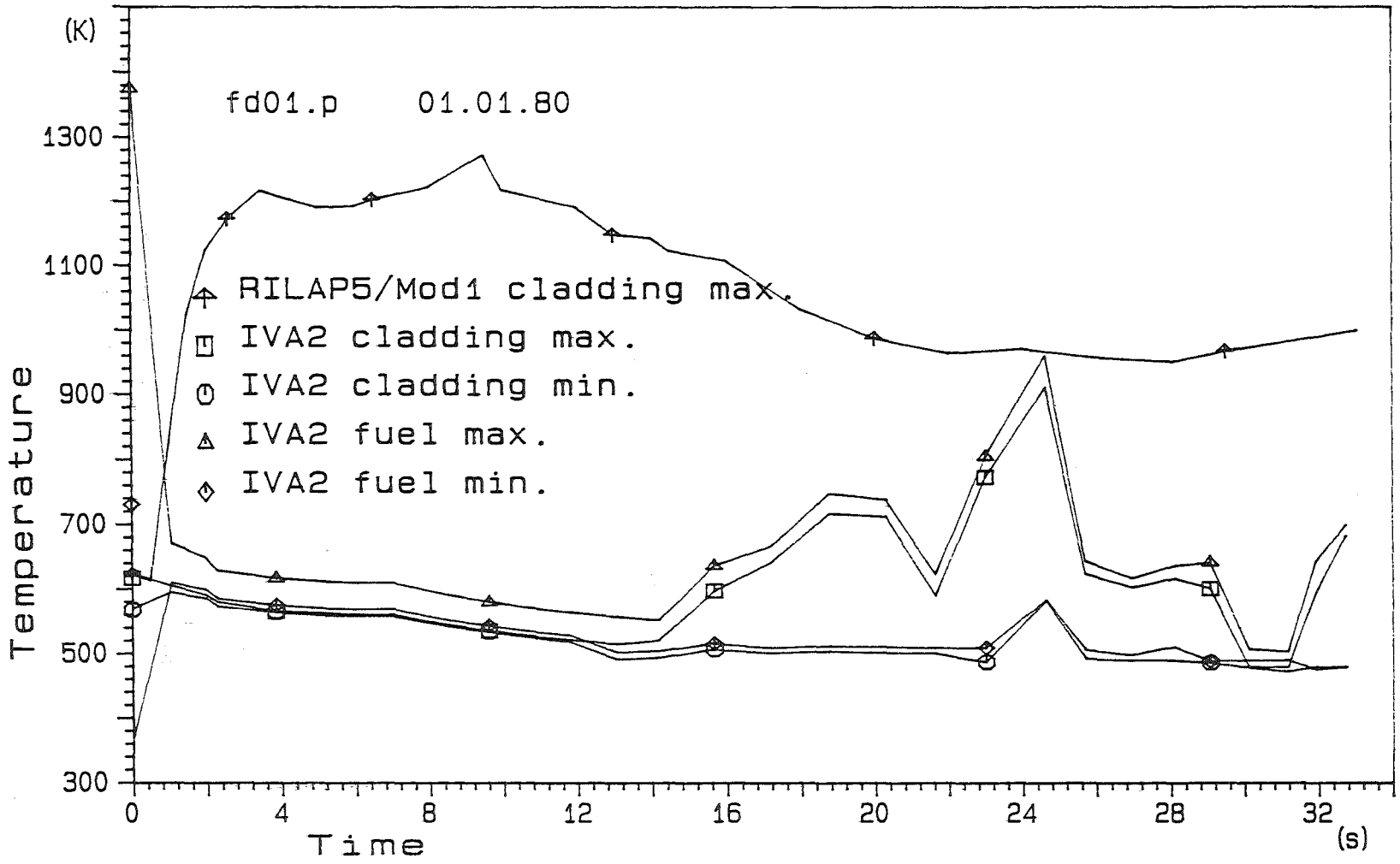

Fig.9 The maximum and the minimum fuel- and cladding surface temperature as a function of the time. IVA2 prediction with form factor=1.35 compared with the RELAP5/Mod1 prediction of the hot spot temperature (hot channel factor= 2.57).

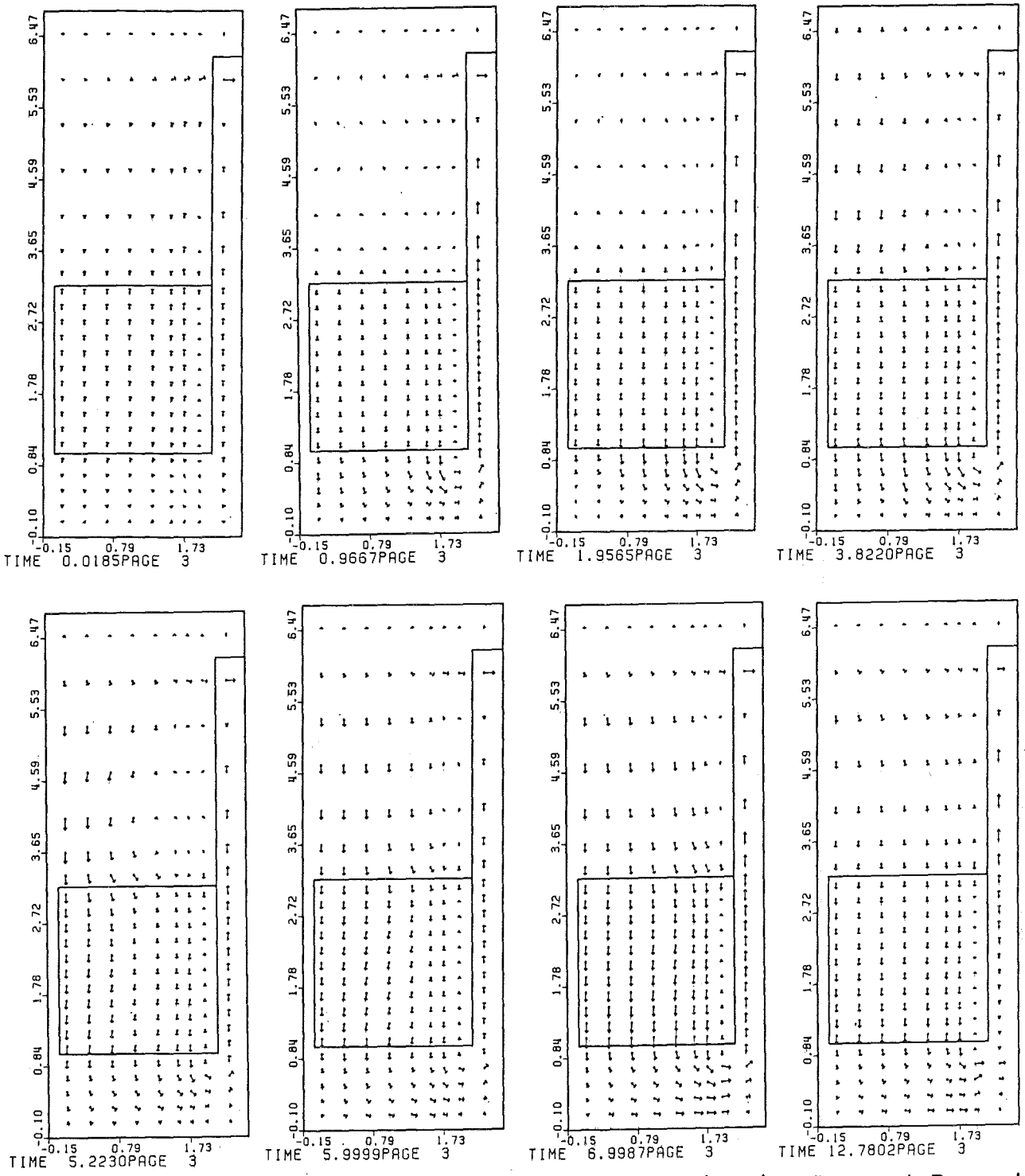

Fig.10 The center of mass velocity in the (r, z)-plane J=3 next to the plane connected with the broken loop.

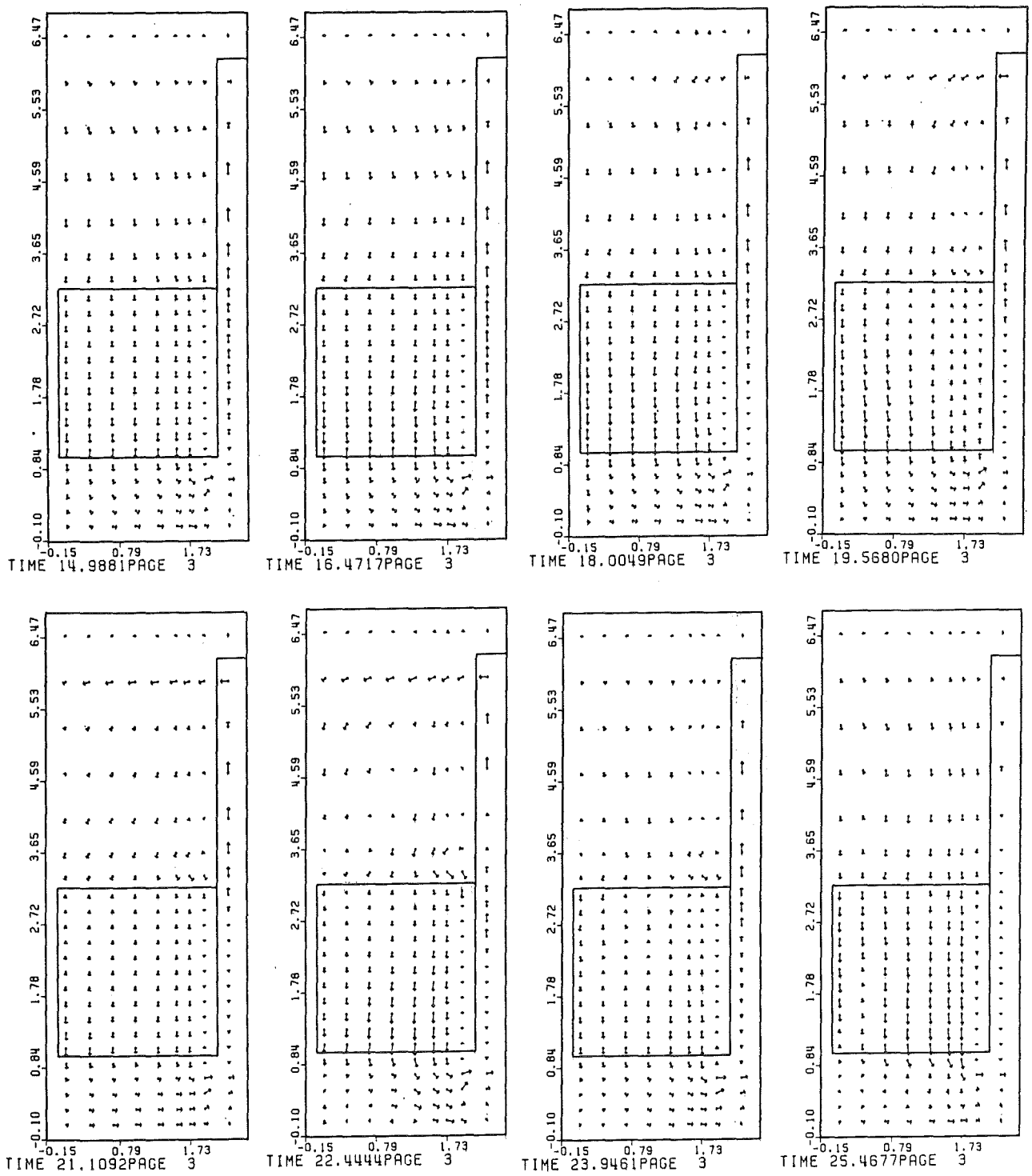

Fig.10 The center of mass velocity in the (r, z)-plane J=3 next to the plane connected with the broken loop.

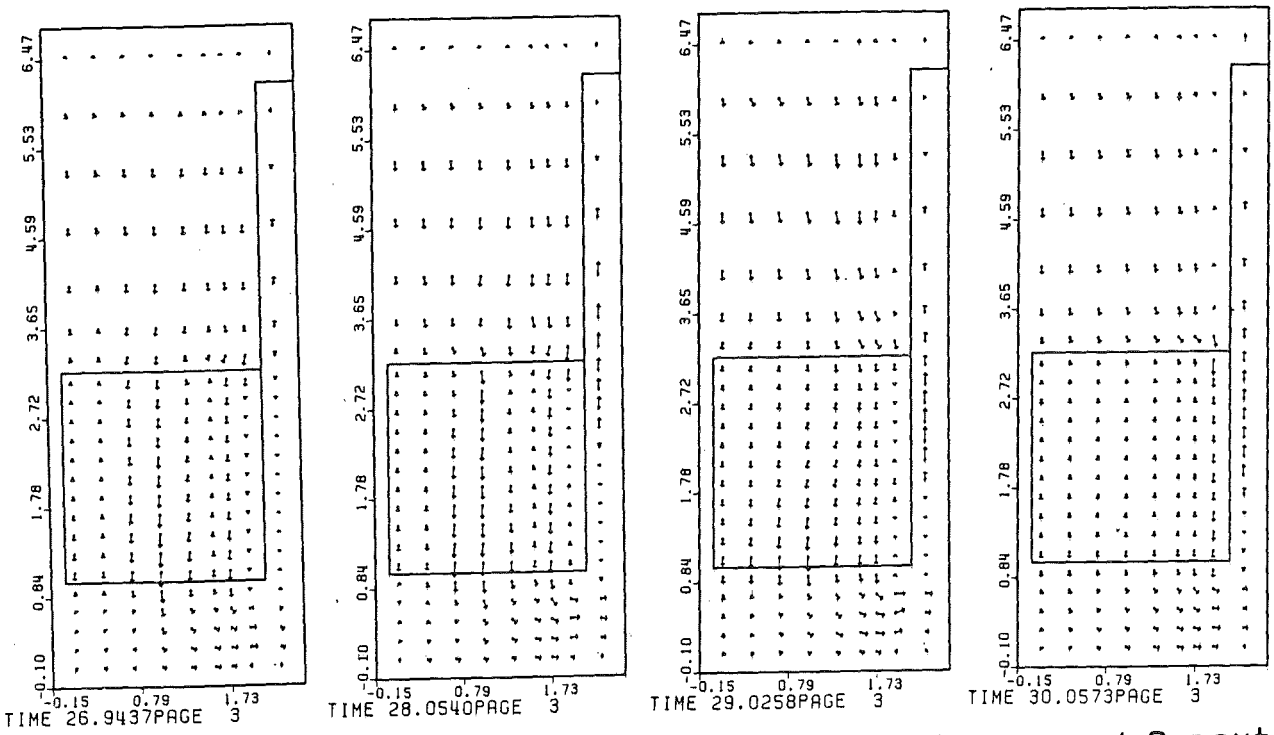

Fig.10 The center of mass velocity in the (r, z)-plane J=3 next to the plane connected with the broken loop.